ELSEVIER

PII: S0032-3861(97)00131-6

Polymer Vol. 38 No. 23, pp. 5725–5733, 1997

0032-3861/97/$17.00+0.00

The γ-phase of high molecular weight isotactic polypropylene. II: The morphology of the γ-form crystallized at 200 MPa

Khaled Mezghani and Paul J. Phillips*

Department of Materials Science and Engineering, University of Tennessee, Knoxville, TN 37996-2200, USA

(Received 12 August 1996; revised 15 January 1997)

The γ-form of isotactic polypropylene, crystallized at elevated pressures, exhibits three distinct classes of spherulites, categorized according to the sign of the birefringence. The results show that at 200 MPa positively birefringent spherulites are observed for crystallization temperatures below 184°C and above 199°C, negatively birefringent spherulites are observed for crystallization in the range 187–198°C and mixed birefringence in the ranges 182–188°C and 196–200°C. In addition, the complex arrangement of the lamellae within these spherulites has been studied using optical and electron microscopy. The results indicate the presence of a hitherto-unreported form of lamellar aggregation, which is best described as feather-like. The birefringence results indicate that the feather-like structure is solely developed by self-epitaxial growth of the γ-lamellae. Melting studies of 'mixed birefringent' spherulites show that the epitaxially grown featherlike structures have higher melting points than radial lamellae grown concurrently in the same spherulite, leading to the inference that it is possible to grow substantial amounts of two different types of lamellae concurrently, that are not distinguishable using conventional wide and small angle X-ray analyses.

(Keywords: polypropylene; crystallization; γ-crystals)

INTRODUCTION

On the crystal lattice level, isotactic polypropylene (iPP) exhibits three different morphological forms, α, β and γ, distinguished by the arrangement of the chains[1–7]. Each of these forms is observed with different preparation procedures[2,6,7] and identified with specific peaks in the X-ray pattern as shown in *Figure 1*.

The γ-form of iPP was first reported during the 1960s and was generated by either crystallization at elevated pressures of the homopolymer or by crystallization at atmospheric pressure of low molecular weight fractions or of copolymers[1,2,8–15]. When varying the pressure both the α- and γ-forms are observed[8,15]. As the crystallization pressure increases the γ-form coexists with the α-form until it becomes dominant at 2 kbar[15]. More recent experimentation[16] has shown that for crystallization at a constant pressure the γ-form is the preferred form at low supercoolings.

All attempts at producing oriented fibres of the γ-form have failed and so identification of its crystal structure has depended on X-ray diffraction studies of powder or bulk samples, although diffraction patterns have been reported of low molecular weight γ-single crystals[17]. The crystal structure was first identified as triclinic[9] with the unit cell being similar to that of the α form, with a slip along the c-axis direction ($a = 6.54$ Å, $b = 21.40$ Å, $c = 6.50$ Å, $\alpha = 89°$, $\beta = 99.6°$, $\gamma = 99°$). However, according to Brückner and Meille[18,19] this structure does not account for the diffraction peak at $2\theta = 24.5°$. Recent studies[18,19] of a form generated at atmospheric pressure from low molecular weight iPP ($M_n = 6300$) led to a reassignment of the structure as a modified triclinic unit cell with lattice parameters $a = 6.55$ Å, $b = 21.57$ Å, $c = 6.55$ Å, $\alpha = 97.4°$, $\beta = 98.8°$, $\gamma = 97.4°$. The main difference between these two unit cells is that the angle α is higher in the modified triclinic cell. Contrary to the previously proposed unit cell, the modified cell accounts for the diffraction maximum at $2\theta = 24.5°$. The lattice parameters of the modified triclinic structure permit the generation of a face-centered orthorhombic unit cell[18,19]. This new structure is unique, in that it contains sheets of parallel molecules, but the molecular orientation between adjacent sheets becomes non-parallel every two sheets (*Figure 2*). The angle between the non-parallel stems is about 81°. This angle is also observed at the contact planes between the radial lamellae and the branches of the α-form[20–26]. Stacks of non parallel chains for low molecular weight iPP, where extended chains are possible, are reasonable.

The main objective of this study is to determine the detailed morphological structure of the γ-form crystallized at elevated pressures. For this reason, morphological studies of the γ-form generated at 200 MPa are conducted using several experimental techniques, namely optical microscopy (OM), scanning electron microscopy (SEM), and atomic force microscopy (AFM).

Using depolarizing light microscopy, several types of spherulite can be distinguished. Usually, the polarizing microscopic pattern of a spherulite shows a central dark

* To whom correspondence should be addressed

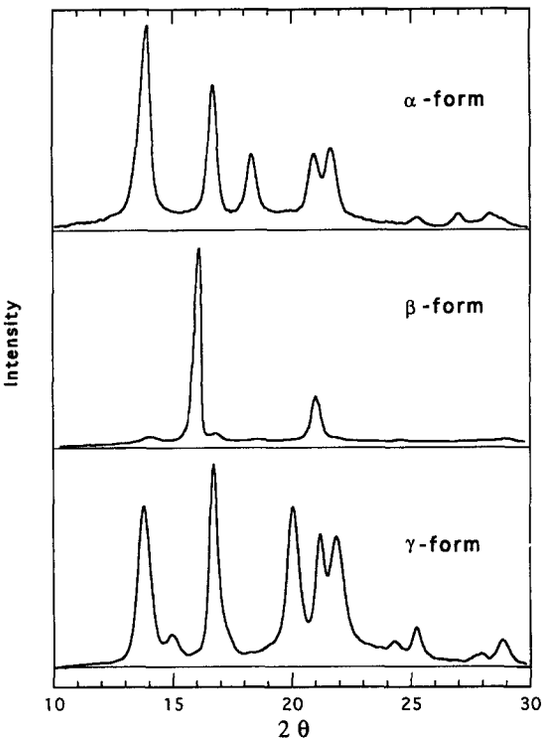

Figure 1 WAXD of different morphological forms of isotactic polypropylene

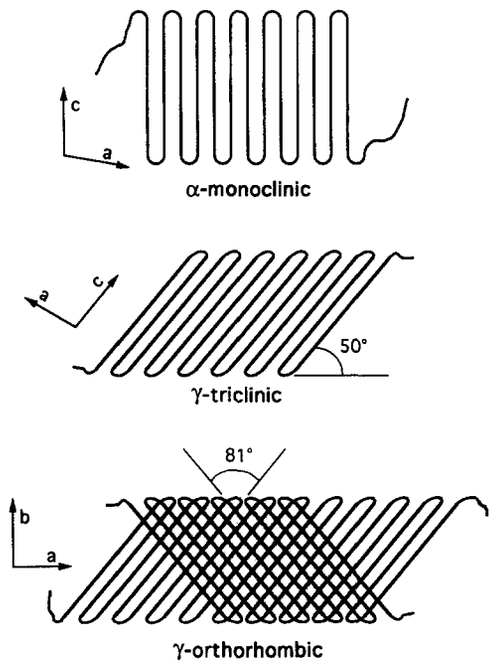

Figure 2 Schematic arrangement of chain stems in the α-monoclinic, γ-triclinic, and γ-orthorhombic unit cells

cross (Maltese cross) with wings coincident with the respective planes of polarizer and analyser. Depending on the birefringence, spherulites can be optically positive or negative[27]. The sign of birefringence of the spherulites can be determined by means of a primary red filter (1/4 λ-plate) located diagonally between crossed polars. When a spherulite is positive, its first and third quarters are blue and the second and fourth ones are yellow, while a reversed arrangement of the quarters is observed for a negative spherulite[28].

So far only preliminary studies of the spherulitic morphology of the γ-form have been reported[15]. In that study experiments were conducted as a function of crystallization pressure at constant supercooling of 50°C. The analysis of the optical studies of microtomed sections showed no evidence of Maltese cross formation when less than 10% of the material was in the γ-form, whereas there was a clear Maltese cross when more than 60% was in the γ-form. Additionally, optical and electron microscope studies of etched specimens revealed no cross hatching in a specimen with >60% γ-crystals. In this paper we will report the results of a comprehensive study of the morphology of γ-spherulites produced at 200 MPa as a function of crystallization temperature in specimens for which only γ-crystals can be detected using wide angle X-ray diffraction. A total of three types of spherulites can be produced using the sign of the birefringence as a classification standard. The studies show that there are two growth mechanisms present, one radial and one tangential, which generate a unique feather structure. Melting studies of pure γ-form show that during melting a mixed type spherulite transforms into a positive type. This transformation is due to the melting of branches, similar to the observed melting of the mixed α-form.

EXPERIMENTAL

Isotactic polypropylene, iPP, was supplied by Exxon Corporation and had molecular weights as follows: M_n 72 000, M_w 257 000, and M_z 528 000. The isotacticity has been determined by Prof. Leo Mandelkern using n.m.r. as an isotactic pentad content of 0.907 whereas structural irregularities are 1.26 mol%. It is the latter figure that is relevant to crystallization studies.

The high pressure crystallization unit is composed of a temperature control unit, a high pressure control unit, and a recording system. The equipment is a modified version of equipment described earlier[15]. The high pressure cell is mounted on a microscope under cross-polar conditions. A binocular is used, with one beam passing to a video camera and one for direct observation. The polymer sample was held between two quartz or sapphire windows inside the pressure cell (*Figure 3*). *In situ* melting studies were conducted at elevated pressures using the transmitted depolarized light intensity method, DLM. First, the sample was melted at 200°C for about 10 min, then rapidly cooled to the desired crystallization temperature. The temperature was

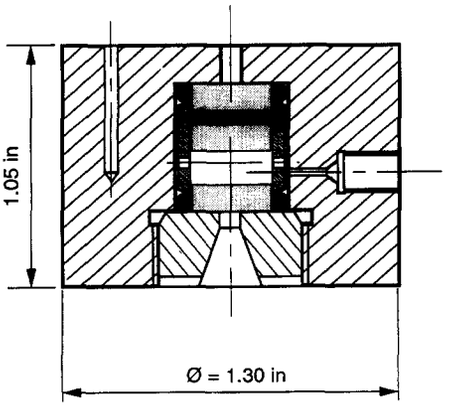

Figure 3 Schematic of the high pressure cell

then allowed to equilibrate using a Mettler controller. After thermal equilibrium was attained the pressure was applied. This procedure assured that the crystallization of samples was conducted isothermally and isobarically. The bulk of the pressure cell limited the maximum heating rate possible to $3°C\,min^{-1}$.

Wide-angle X-ray diffraction (WAXD) studies were carried out using a Rigaku Denki diffractometer. Samples were prepared isothermally for analysis in the high pressure cell at 200 MPa (2.0 kbar), but studied using X-rays at atmospheric pressure. A 10 μm thick sample was prepared at 200 MPa and 203°C for studies using the atomic force microscope (AFM), reflection optical microscope (ROM), and scanning electron microscope (SEM). The sample was permanganically etched for 30 min[4] and lightly coated with chromium for SEM studies. AFM studies were carried out on an instrument at Oak Ridge National Laboratory using the tapping mode with a scan rate of 1.174 Hz.

RESULTS

The composition of any specimen can be determined with good accuracy from WAXD results. Each of the α, β and γ crystal forms has a distinctive peak in the WAXD plots even though many of the peaks are in similar locations preventing deconvolution of entire spectra into the component parts. These characteristic peaks are found in the 2θ plot between the angles (18–19°) and (19.2–20.5°) for α and γ crystals respectively. In the absence of structure factors and other corrective information, the ratio of the areas under these two peaks has been taken as a measure of the relative proportions of the two phases. The results of the WAXD experiments indicate that 100% γ-form is present in samples crystallized above 176°C (*Figure 4*) and that the sample is more than 65% crystalline.

On the spherulitic level, the 100% γ-form exhibits a variety of spherulite types classified according to the sign of the birefringence. This has been determined through the use of a primary red filter (1/4 λ-plate) located diagonally between crossed polars. When iPP was crystallized in the temperature range 176–206°C three distinct types of spherulite were identified, the data being summarized in *Table 1*. Negatively birefringent spherulites γ_n, were observed in the temperature range of 187–198°C (*Figure 5*). These spherulites showed quite distinctive Maltese crosses and also a relatively high density of nucleation. Positively birefringent spherulites, γ_p, were generated in two temperature regions, below 184°C and above 199°C (*Figure 6*). The spherulites which were developed above 199°C exhibit clear Maltese crosses and tend to be large with a clear fibrous texture on a significant scale. However, at temperatures below 184°C the nucleation density was so high and the growth rate was so fast

Table 1 Classification of the γ-form spherulites at 200 MPa

Spherulite type	γ_p	γ_m	γ_n	γ_m	γ_p
Sign of birefringence	+ve	Mixed	−ve	Mixed	+ve
Crystallization temperature (°C)	<184	182–188	187–198	196–200	>199

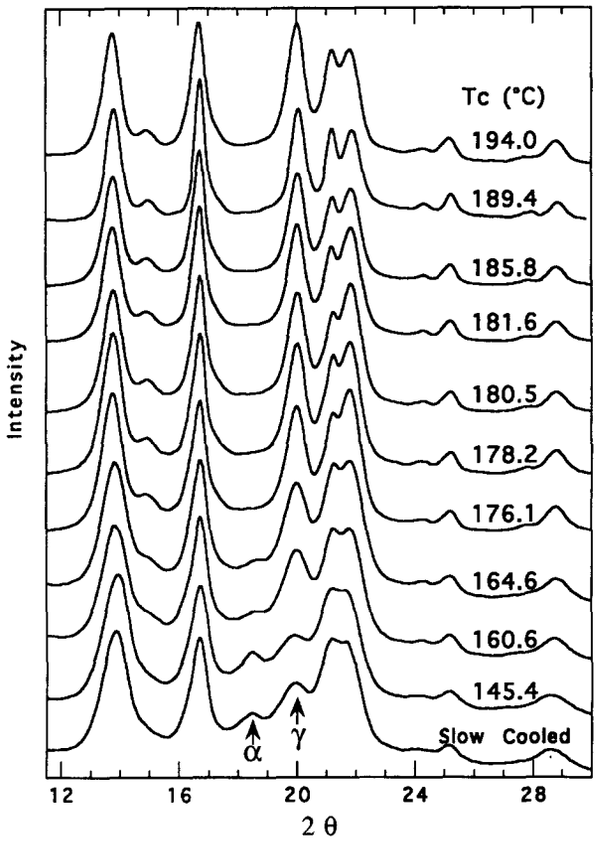

Figure 4 WAXD of iPP isothermally crystallized at 200 MPa (2.00 kbar)

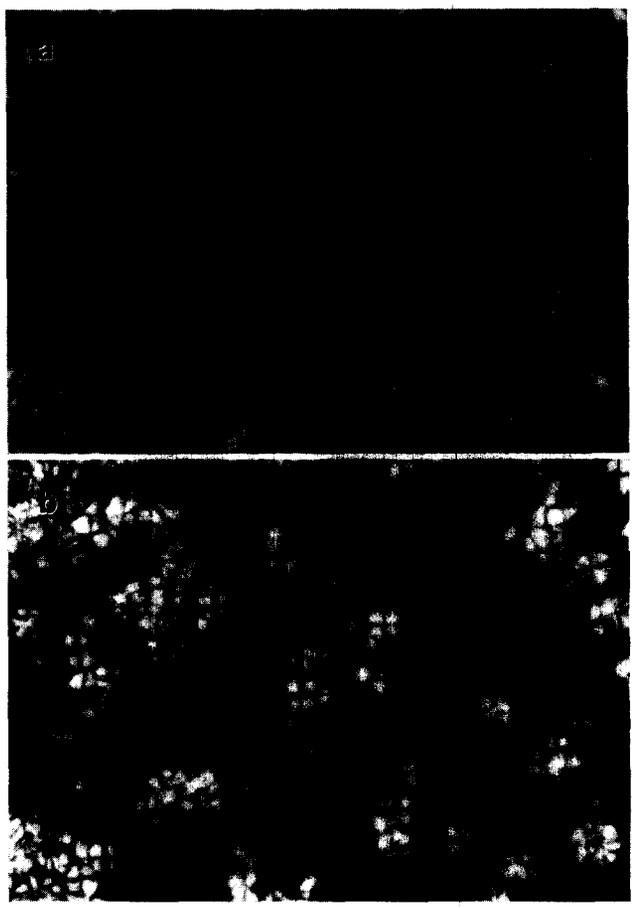

Figure 5 Negative birefringence spherulites, γ_n, prepared at 200 MPa and isothermal crystallization temperature of 190°C. (a) With red filter (1/4 λ-plate); (b) without red filter

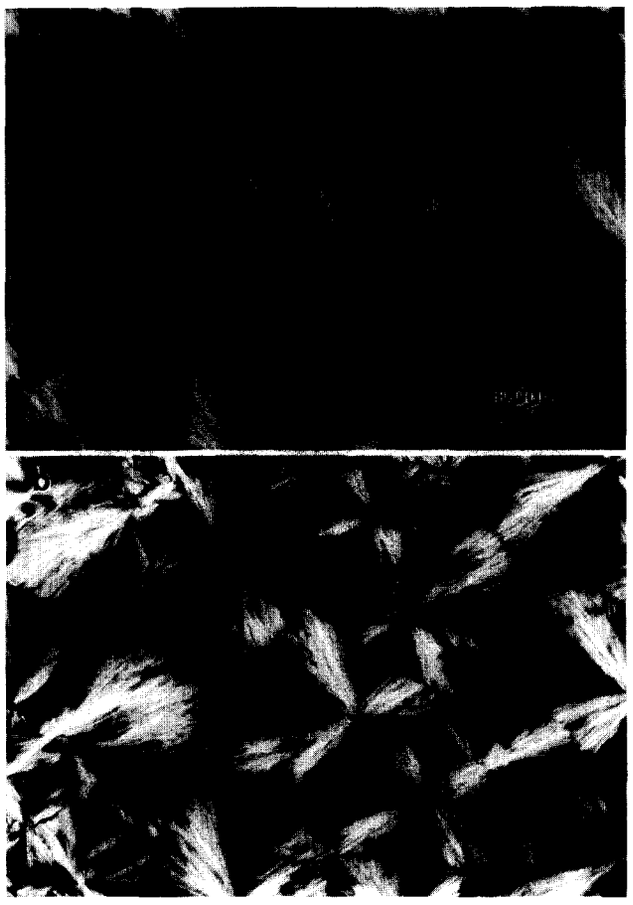

Figure 6 Positive birefringence spherulites, γ_p, prepared at 200 MPa and isothermal crystallization temperature of 205°C. The crystallization time is 45 h. (a) With red filter (1/4 λ-plane); (b) without red filter

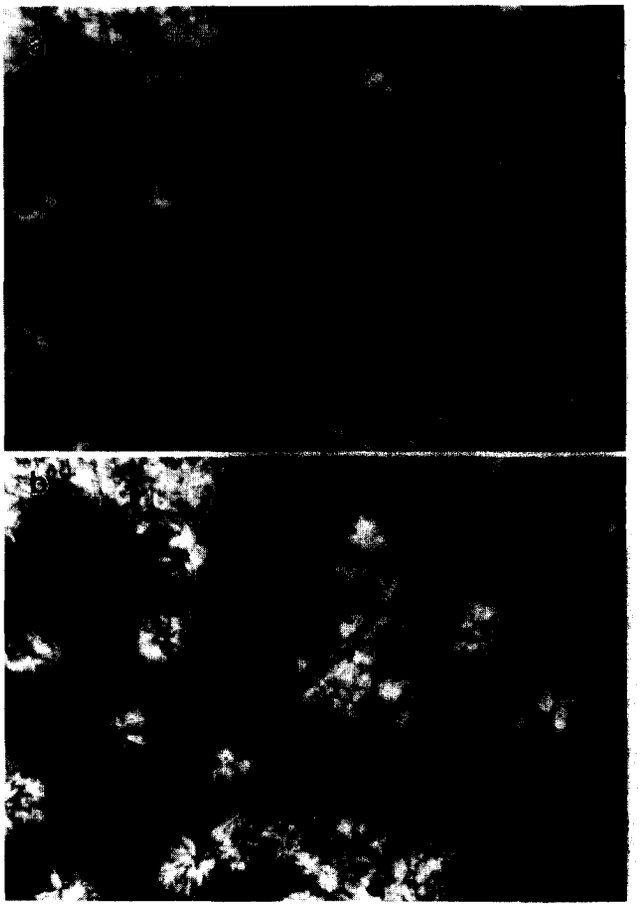

Figure 7 Mixed birefringence spherulites, γ_m, prepared at 200 MPa and isothermal crystallization temperature of 198°C. (a) With red filter (1/4 λ-plate); (b) without red filter

that clear micrographs were not possible. The third type, illustrated in *Figure 7*, was termed 'mixed birefringence', γ_m, because of its lack of clearly discernible coloured quadrants. Although there were occasional complete or partial quadrants observable, these structures more closely resembled axialitic species. Although approximately spherical in shape, there was little evidence for a dominant radial growth habit. This type of spherulite was observed in the temperature ranges of 182–188°C and 196–200°C.

In situ melting studies of these three types of spherulites were conducted at 200 MPa. Even though the analyses were conducted for all crystallization temperatures, the changes of birefringence of the high supercooling samples were not obvious, partly because of the high nucleation density in the samples. What is reported here is the observed melting of samples crystallized above the temperature of 195°C, where relatively large spherulites were developed. It was observed that during melting the mixed birefringence spherulites became positive, as illustrated in *Figure 8*. This was in contrast to the positive and negative spherulites, both of which retained the sign of their birefringence until completely melted. This lack of change suggested that, unlike the situation in α-spherulites, the birefringences of the γ_n and γ_p are not a result of branching content, but must be caused by something more fundamental in origin.

In order to investigate the structure of the spherulites in greater detail, studies at the lamellar level were conducted. It is well established that iPP forms lamellar structures regardless of whether it is crystallized under quiescent or stress-induced conditions[4,29–31]. For any detailed analysis of the lamellar structure, a polymeric sample had to be etched. For this purpose a sample totally crystallized at 200 MPa and 203°C, hence containing positively birefringent spherulites, was permanganically etched for 30 min. As observed in unetched samples and transmitted light (*Figure 6*), spherulites can be discerned clearly. The boundaries are easily observed at low magnification in etched samples with reflected light (*Figure 9*). When studied at higher levels of magnification a completely new structure can be observed (*Figure 10*), demonstrating that each of these spherulites is composed of distinct feather-like structures radiating approximately radially from the centres of the spherulites. This feature, which has never been reported for any polymer, is unique to the γ-form. SEM studies reveal more details of the internal structure of the 'feathers' (*Figure 11*) where it is seen that the individual lamellae are inclined at an angle that is near 70° to the radial direction comprising the backbone of the feather. Occasionally other morphological features can be seen, for instance illustrated in *Figure 12* is an example of a 'feather' either bifurcating to form two main branches or generating a branch from within itself.

The sample which was prepared for reflection optical microscopy and SEM studies was also analysed using atomic force microscopy. The AFM is capable of delivering more depth of contrast and an estimate of

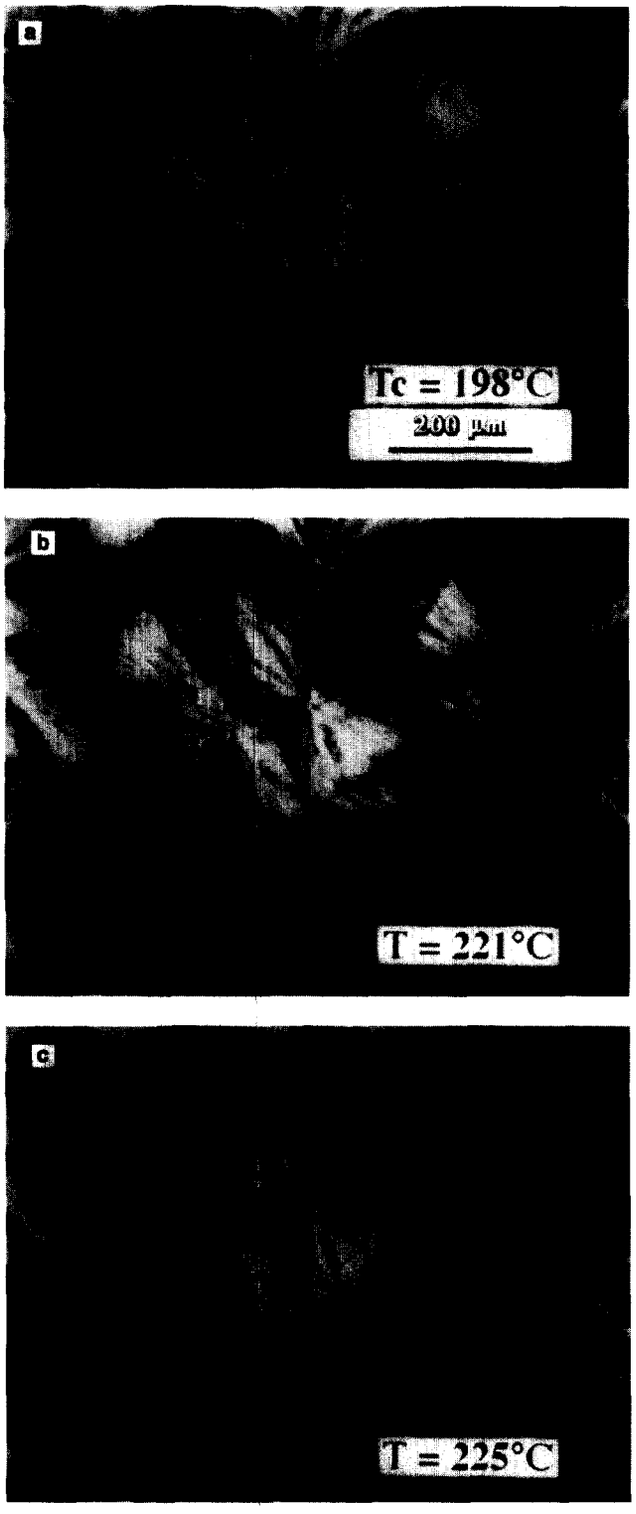

Figure 8 During melting, mixed birefringence spherulites, γ_m, become positive. (a) Isothermal crystallization temperature of 198°C and at 200 MPa; (b) during melting, $T = 221$°C; (c) during melting, $T = 225$°C

the depth of the lamellar features making up the 'feather'. Typical micrographs are shown in *Figures 13* and *14*, where it can be seen that the features observed using optical and scanning microscopy are repeated and that the feathers are relatively flat and composed of stacks of lamellae. The average lamellar thickness of this sample can be calculated from SAXS studies to be 15.7 nm, whereas the average measured thickness of stacks of lamellae varies between 100 and 500 nm. Simple

Figure 9 Reflection optical micrograph of spherulites in iPP crystallized at 200 MPa and isothermal crystallization temperature of 203°C. The sample was permanganically etched for 30 min

Figure 10 Reflection optical micrograph of feather-like structure in iPP spherulites. Magnification of *Figure 9*

Figure 11 SEM micrograph of lamellae crystallized at 200 MPa and 203°C. Same sample as of *Figure 9*. The sample was permanganically etched for 30 min and lightly coated with chromium. The growth of lamellae is near tangential to the growth of the spherulite, moreover, lamellae are arranged in a feather-like structure

Figure 12 SEM micrograph of lamellae crystallized at 200 MPa and 203°C. The growth of lamellae is near tangential to the growth of the spherulite

Figure 13 AFM micrograph of lamellae crystallized at 200 MPa and 203°C. Lamellae are arranged in a feather-like structure. The sample was permanganically etched for 30 min

division shows there to be approximately 20 lamellae in each stack leaving the axis of the feather. A more detailed analysis is presented in *Table 2*.

Optical micrographs of the feather-like structures at different magnifications are presented in *Figures 15–17*, where the details of the birefringence can be seen. The

Figure 14 Three dimensional (3-D) imaging of *Figure 13*

Table 2 Average number of lamellae in several stacks in the microscope

Experimental technique	Magnification	Average stack thickness (nm)	Average number of lamellae in a stack
Reflection light microscopy	High	430	27
Scanning electron microscopy	High	110	7
Atomic force microscopy	Low	480	30
	High	275	17

Note: The average lamellar thickness was determined from small angle X-ray scattering technique to be 15.7 nm

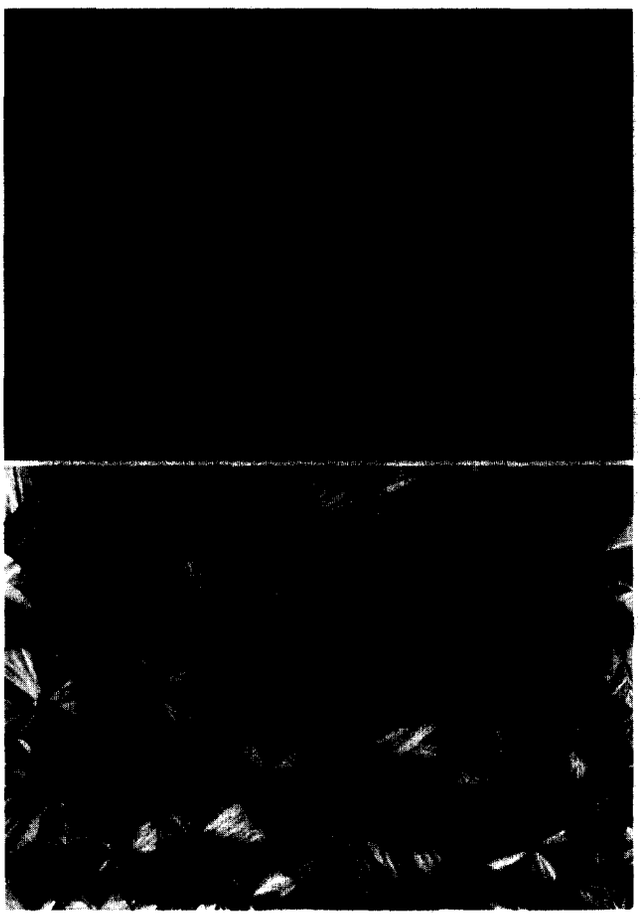

Figure 15 Feather-like structure of the γ-form; (a) with red filter (1/4 λ-plate); (b) without red filter

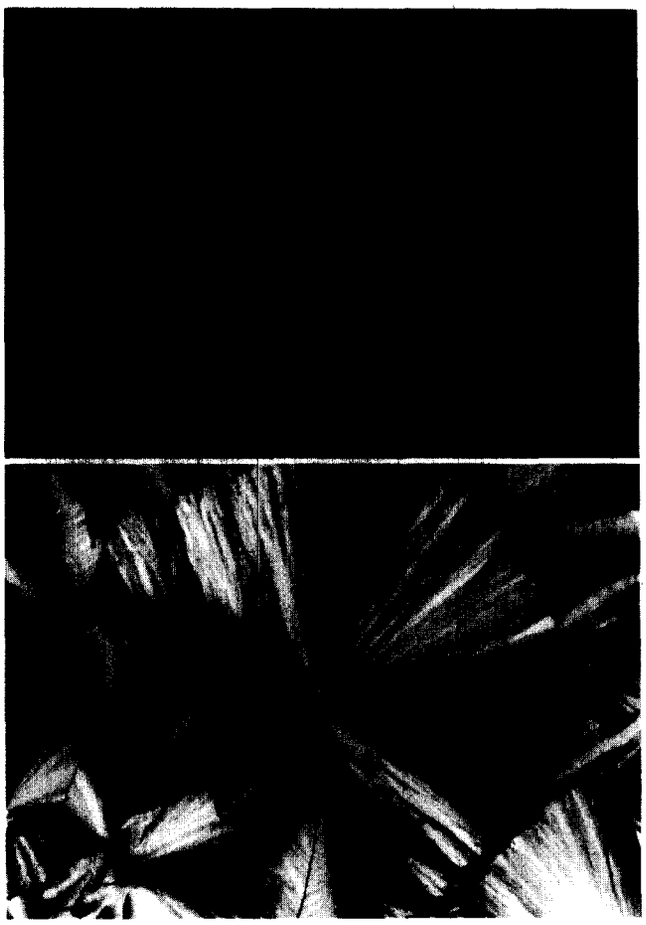

Figure 16 Feather-like structure of the γ-form. Same sample as *Figure 15*; (a) with red filter (1/4 λ-plate); (b) without red filter

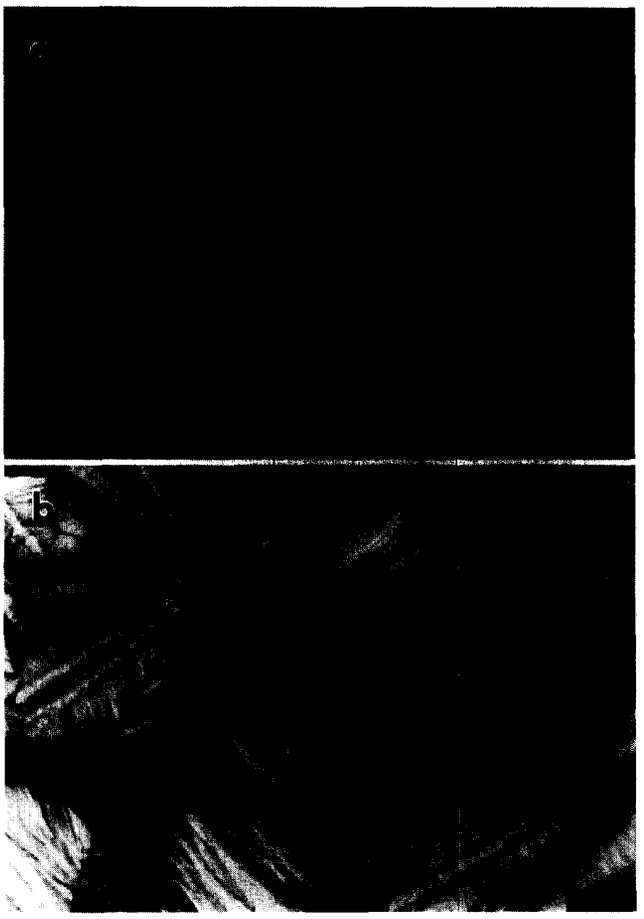

Figure 17 Feather-like structure of the γ-form. Same sample as *Figures 15* and *16*; (a) with red filter (1/4 λ-plate); (b) without red filter

sample was prepared as a very thin film (less than 1 μm) at 200 MPa and an isothermal crystallization temperature of 188°C.

DISCUSSION

The results show clearly that γ-polypropylene forms three different types of spherulite, on the basis of sign of birefringence, as a function of crystallization temperature. Positively birefringent spherulites are observed at both high and low supercoolings, with negatively birefringent species occurring at intermediate supercoolings. The relation between these structures and crystallization kinetic regimes will be discussed in a later paper. The transition zones between the negatively birefringent and positively birefringent species are characterized by the concurrent growth of spherulites with no clearly discernible sign of birefringence, which have been labelled 'mixed birefringence' spherulites. Melting studies of the latter species grown in the vicinity of the higher temperature transition showed that they converted into clearly positively birefringent spherulites during the melting process. This effect indicates an overgrowth of lower melting point branched species, which when melted permit the dominant positively birefringent undergrowth to be seen.

Negatively birefringent spherulites are the normal growth mode in classical spherulitic growth where the dominant lamellae grow in an approximately radial manner. Branches are expected to leave the dominant lamellae at an acute angle, the largest angle known for polypropylene being that associated with the 'cross-hatched' overgrowth of α-lamellae due to the presence of a relatively unique epitaxial relationship. It is well known that the change of birefringence in α-spherulites with crystallization temperature is directly related to the amount of lamellae generated by that specific branching mechanism. However, in the case of γ-spherulites the change of birefringence is due to two different lamellar growth mechanisms, comprising conventional radial lamellar growth and complex epitaxially grown branched structures. Surprisingly, it is the radial lamellar growth patches that melt out first in mixed growth spherulites, leaving as the more stable species the lamellae that comprise the feather-like structures giving rise to the positively birefringent growth.

Furthermore, in classical spherulitic structures the dominant radial lamellae tend to dominate at the lowest supercoolings (e.g. the axialites in regime I of polyethylene), yet here they are only seen at intermediate supercoolings. The generation of positively birefringent spherulites at the lowest possible supercoolings is unexpected and suggests a quite unique occurrence. Growth at the lowest supercoolings is always regarded as the closest possible to equilibrium structure formation, yet here it is occurring in a form that is not constituted of radiating dominant lamellae.

It is the form of these positively birefringent feather-like epitaxial species that has received particular attention in our studies. Clearly it was necessary to elucidate

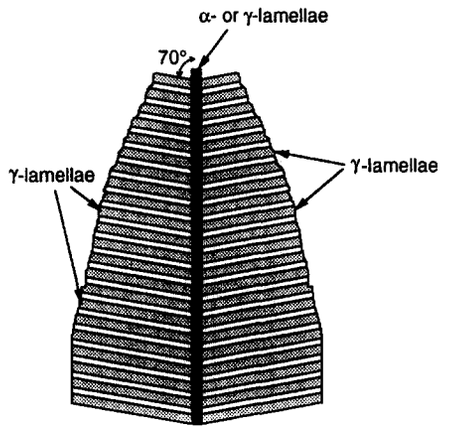

a) Epitaxial growth of γ-lamellae on α- or γ-lamellae

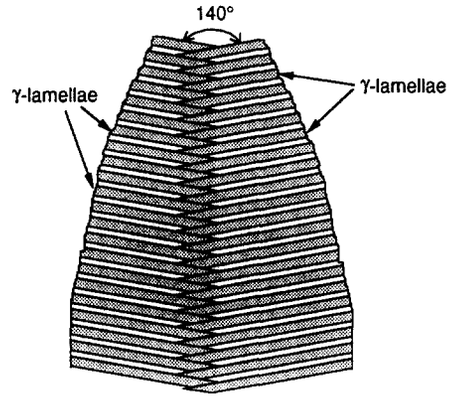

b) Epitaxial growth of γ-lamellae on γ-lamellae

Figure 18 Schematic representation of the potential growth mechanisms of the feather-like structure

as much information as possible on the formation of these fascinating structures in order to be able to begin to hypothesize on the reasons why such an epitaxial growth should have a higher melting point than radiating lamellae grown concurrently.

There are two possible schemes for the growth of lamellae in the feather-like structure: (i) branching of γ-lamellae on a radially grown γ- or α-lamella at an angle of *ca.* 70° as indicated in *Figure 18a*; (ii) growth of γ-lamellae at an angle of *ca.* 140° on previously grown γ-lamellae, as shown in *Figure 18b*.

Strong evidence for both growth schemes was obtained from RLM, SEM, and AFM micrographs, some of which were reported in the Results section. For example, at low resolution (*Figure 10*) the feather-like structure appears to follow the growth mechanism of *Figure 18a*. This appearance may be due to poor etching of the sample in certain areas. On the other hand, observations of well etched regions at higher magnifications, such as in *Figure 12* indicate that the growth mechanism of *Figure 18b* is more suitable since radial lamellae cannot be detected in the middle of the feather-like structure. However this observation might be due to overetching of that region removing radial lamellae. Another explanation could be that radial lamellae were located below the branches and so could not be observed. These arguments might be resolved in the future through transmission electron microscopy (TEM) of the growth tips of the feather-like structure.

The WAXD pattern shows no evidence of the α-peak in the 2θ range of 18–19°. In earlier studies we have measured 3% of α without any problem and believe that 1%, or even less, could be detected using this simple ratio of areas approach. Of course, whether the value calculated using this approach is the true value cannot be answered without structure factor calibrations, which are not available for these crystals. Even so, it is possible that less than 1% of this form, if it existed, would not be detected using WAXD; therefore, the possibility of the α-form being the main radial lamellae of the feather-like structure cannot be totally ignored. Several examples of the 'feathers' in the micrographs of *Figures 15* and *17* apparently show that the axial widths of the feathers' axes occupy more than 10% of the total area of the sample. Ten per cent of α-form would have been easily detected as a small peak in the angle range 18–19°. On the other hand, examination of *Figure 17* shows that the birefringence of the central axis of the feather-like structure is positive. Good examples of this feature can be seen in the third quadrant where there are two adjacent feathers on the left side of the picture, or the single feather at bottom right. Accordingly, the birefringence of all parts of these feathers is positive. If the feather axis were composed of α-lamellae then its birefringence would be negative. Consequently, it seems most likely that the central axis is composed of γ-material, the only possibility of an α-axis being if it were so small as to be undetectable in WAXD, and at the same time, totally enveloped in positively birefringent branches of γ-lamellae so as that its birefringence sign could not be seen in optical microscopy studies.

WAXD studies indicated clearly the total dominance of γ-crystals in the specimens reported in this paper. Yet, in the case of the 'mixed birefringent' samples there are clearly two concurrent populations of γ-crystals of substantially different melting points and SAXS studies, to be reported in detail later, show no evidence for the presence of two populations of crystal thickness. There are several possible explanations for two sets of apparently identical lamellae having different melting points. From a crude examination of the melting equation, it is apparent that differences in surface free energy are a likely origin. These would of necessity be caused by different fold structures or by different levels of frozen-in strain. However, it is difficult to think of sensible reasons for uniform differences of this nature being present without there being a change of crystal structure, since the crystals are growing concurrently under identical conditions in the same film, and within the same spherulites. It is always possible that the negatively birefringent and positively birefringent regions differ only in the orientation of the unit cell relative to the spherulitic growth direction. There are instances of this type of behaviour in the literature; for instance Magill[32] and Khoury[33] discuss this possibility and Lovinger found this to be the case for directionally solidified polyamides[34,35]. However, this would not explain the difference of almost 10°C in the melting points of the crystals, unless there were major changes in surface free energy produced by the change of growth face. Another possible explanation is that there are indeed two different crystal forms present, both appearing as γ-crystals. Such a possibility is not a

wild speculation, since the studies of Brückner and Meille[18,19] show that the modified triclinic and the orthorhombic structures both fit the X-ray diffraction results. This fit is appropriate regardless of whether the polymer is the low molecular weight form of their original studies[18,19] or specimens prepared by ourselves from high molecular weight polymer at 185.8°C and 200 MPa, similar to some of the low supercooling conditions reported in this paper[36]. Further explanation and discussion of the true nature of the phenomenon must await further analyses and experimentation.

CONCLUSIONS

When analysing the birefringence changes at the spherulitic level as a function of crystallization temperature at 200 MPa, the γ-form exhibited three distinct types of spherulites. A negative birefringence type, γ_n, was developed in the range of 187–198°C, whereas, a positive type, γ_p, was generated above 199°C and below 184°C. The third type, mixed birefringence (γ_m), was observed in the ranges of 182–188°C and 196–200°C.

The results of reflection optical microscope, SEM, and AFM studies showed that positive spherulites grown in the upper temperature range were composed of a unique feather-like structure. This feature, which has never been reported for any polymer, is unique to the γ-form. In addition, the SEM, the AFM, and the birefingence results indicated that the feather-like structure was solely developed by self-epitaxial growth of the γ-lamellae.

From the morphological studies, it was demonstrated that two distinct growth mechanisms generate the γ-form. The first one, conventional radial growth accounts for the negative birefringent species. The second one, the tangential or feather-like growth is the source of the positive spherulites. A mixture of these two types, radial and feather-like, developed the mixed type birefringence, which was a transition region between the negative and the positive birefringence regions.

Melting studies of the 'mixed birefringent' spherulites indicate that the radial lamellar patches melt at a lower temperature than the concurrently grown epitaxial feather-like structures, suggesting that the feather-like epitaxial species are the more stable form. The differences between the two forms of crystal are not known at this time.

ACKNOWLEDGEMENT

Financial support from the Polymers Program of the National Science Foundation through grants DMR910-7675 and DMR9408678 is gratefully acknowledged.

REFERENCES

1. Addink, E. J. and Beintema, J., *Polymer*, 1961, **2**, 185.
2. Turner-Jones, A., Aizlewood, J. M. and Beckett, D. R., *Makromol. Chem.*, 1964, **75**, 134.
3. Binsbergen, F. L. and Lange, B. G. M., *Polymer*, 1968, **9**, 23.
4. Norton, D. R. and Keller, A., *Polymer*, 1985, **26**, 704.
5. Awaya, H., *Polymer*, 1988, **29**, 591.
6. Brückner, S., Meille, S. V., Petraccone, V. and Pirozzi, B., *Prog. Polym. Sci.*, 1991, **16**, 361.
7. Varga, J., *J. Materials Sci.*, 1992, **27**, 2557.
8. Kardos, J. L., Christiansen, J. L. and Baer, E., *J. Polym. Sci. (A-2)*, 1966, **4**, 777.
9. Morrow, D. R. and Newman, B. A., *J. Appl. Phys.*, 1968, **39**, 4944.
10. Pae, K. D., Morrow, D. R. and Sauer, J. A., *Nature*, 1966, **211**, 514.
11. Awaya, H., *J. Polym. Sci., Polym. Lett.*, 1966, **4**, 127.
12. Pae, K. D., *J. Polym. Sci.*, 1968, **6**, 657.
13. Sauer, J. A. and Pae, K. D., *J. Appl. Phys.*, 1968, **39**, 4959.
14. Turner-Jones, A., *Polymer*, 1971, **12**, 487.
15. Campbell, R. A., Phillips, P. J. and Lin, J. S., *Polymer*, 1993, **34**, 4809.
16. Mezghani, K., Ph.D. thesis, University of Tennessee, 1996.
17. Lotz, B., Graff, S. and Straupé, C., *Polymer*, 1991, **32**, 2902.
18. Brückner, S. and Meille, S. V., *Nature*, 1989, **340**, 455.
19. Meille, S. V., Brückner, S. and Porzio, W., *Macromolecules*, 1990, **23**, 4114.
20. Lotz, B. and Wittmann, J. C., *J. Polym. Sci.: Polym. Phys.*, 1986, **24**, 1541.
21. Sauer, J. A., Morrow, D. R. and Richardson, G. C., *J. Appl. Phys.*, 1965, **36**, 3017.
22. Lotz, B. and Wittmann, J. C., *Makromol. Chem.*, 1984, **185**, 2043.
23. Lotz, B. and Wittmann, J. C., *J. Polym. Sci.: Polym. Phys.*, 1986, **24**, 1559.
24. Lotz, B., Graff, S. and Wittmann, J. C., *J. Polym. Sci.: Polym. Phys.*, 1986, **24**, 2017.
25. Wittmann, J. C. and Lotz, B., *J. Polym. Sci.: Polym. Phys. Ed.*, 1985, **23**, 205.
26. Lotz, B., Wittmann, J. C., Stocker, W., Magonov, S. N. and Cantow, H. J., *Polymer Bulletin*, 1991, **20**, 209.
27. Wunderlich, B., *Macromolecular Physics*, Vol. 1. Academic Press, New York, 1975.
28. Haudin, J. M., in *Optical Properties of Polymers*, ed. G. H. Meeten. Elsevier Applied Sci., New York, 1986.
29. Kojima, M., *J. Polym. Sci.*, 1968, **A2** (6), 1255.
30. Bassett, D. C. and Olley, R. H., *Polymer*, 1984, **25**, 935.
31. Padden, F. J. and Keith, H. D., *J. Appl. Phys.*, 1959, **30**, 1479.
32. Magill, J. H., *J. Polym. Sci.*, 1966, **A2** (4), 243.
33. Khoury, F., *J. Polym. Sci.*, 1958, **33**,. 389.
34. Lovinger, A. J., *J. Appl. Phys.*, 1978, **49**, 5003.
35. Lovinger, A. J., *J. Appl. Phys.*, 1978, **49**, 5014.
36. Meille, S. V., Brückner, S., Phillips, P. J. and Mezghani, K., *Macromolecules*, 1996, **29**, 795.